#13.

Thin film Transistors (TFTs)

Materials:

material	mobility (cm^2/Vs)
a-Si:H (n only)	0.6 – 1
poly-Si, n	50 – 400
poly-Si, p	15 – 70
organics, p (n-channel materials are being developed)	10^{-3} – 10

Why are these lousy materials needed?

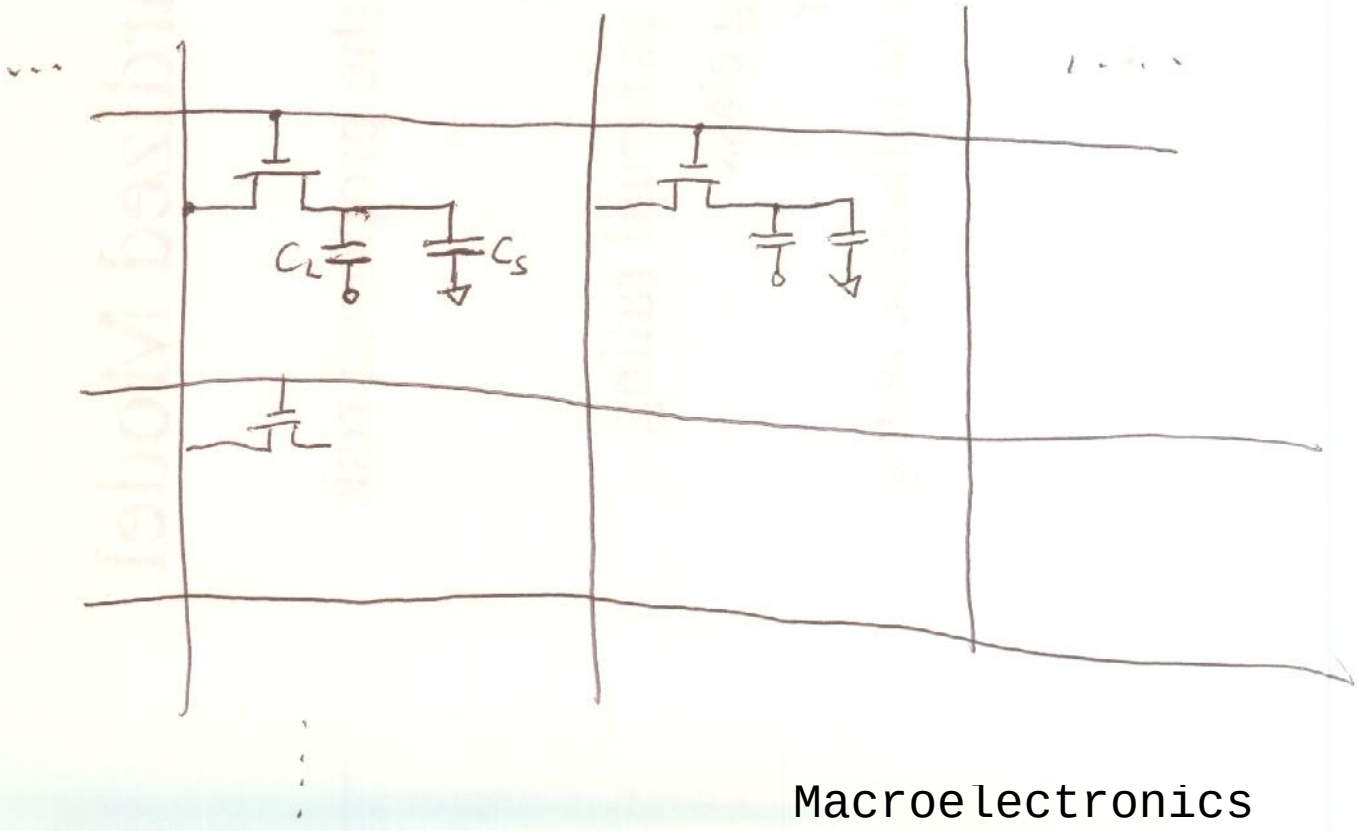

Amorphous Si — a-Si:H

- Tetrahedral bonding in Si
- Due to sp^3 hybridization.
- Local order (tetrahedral) largely unchanged (long range disorder)
- Band structure similar to c-Si

Bonding $\Longleftrightarrow$ Valence band

Antibonding $\Longleftrightarrow$ Conduction band

- But, due to lack of long range order (periodicity), there's no such thing as k!
  - No Bloch theorem.
  - No translational symmetry.

Amorphous Silicon Electronics

R.A. Street

Introduction

The progressive miniaturization of electronics is familiar to everyone; computing power that used to occupy a room can now be put onto a single integrated circuit. Miniaturization is admirable when size is not relevent to the electronic function, but there are plenty of devices in which a large physical size is essential. Many of these concern information technology, examples being the computer display, printer, and fax machine. Communication with the electronic world is primarily visual and operates at a large format typified by a document. In this rapidly advancing field, we are eagerly awaiting desktop interactive display surfaces that can input as well as display information, document readers, truly portable computers, electronic vision and—the oldest dream of all—the television that hangs on the wall. Realization of these hopes requires a set of technologies that permit bigger rather than smaller electronic systems, and amorphous silicon is helping to make this happen.

Crystalline silicon does not cope well with the large sizes needed for electronics at the human interface. Of the many technologies used in present devices, the CRT is the oldest and most successful for displays, printers use moving heads or spinning mirrors, and many other devices use optical projection. Large-area electronic devices add a new dimension to this crowded field. These use circuits similar to those in crystalline silicon but made by the square foot rather than the square inch. Such devices are based on thin-film semiconductors deposited on a convenient substrate, avoiding the necessity of growing large single crystals.

Hydrogenated amorphous silicon (a-Si:H) has existed in its present form for about 20 years,[1] and has made the transition from experimental curiosity to standard material, with broad applications in solar cells, displays, printers, and imaging devices. The first commercial amorphous silicon devices were photovoltaic solar cells, which in 1980 were introduced by Sanyo into consumer products such as handheld calculators. As the efficiency of devices increases, and manufacturing costs decrease, the goal of employing photovoltaic power on a large scale becomes more achievable. Today, amorphous silicon is being used as a photoreceptor in copiers, utilizing the ability to deposit the material over large areas. The most exciting and rapidly growing technological developments in this area, however—and the focus of this paper—are the matrix-addressed arrays. These are multiple pixel devices used for imaging and display. Amorphous silicon optical scanners were first introduced into fax machines in the mid-1980s and now comprise about half the market. Mass production of liquid crystal displays driven by amorphous silicon transistors began in 1987, and their development is particularly rapid now. The prospects for large-area detector devices, including medical x-ray imaging, appear attractive.

The application of amorphous semiconductors to large-area electronics is not new. Selenium photoreceptors enabled the first Xerox copier machines 35 years ago. What is new is the extra functionality provided by the matrix-addressed silicon arrays, which permits electronic reprographics and display in a way not possible with the simple photoreceptor.

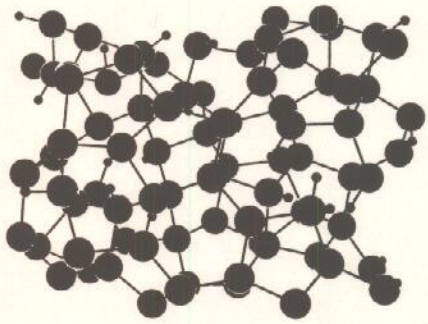

Figure 1. Model of the atomic structure of a-Si:H illustrating the bonding disorder and the presence of hydrogen. Large disks represent silicon atoms and small disks are hydrogen.

Amorphous Silicon

Amorphous silicon is deposited from silane gas (SiH_4) by plasma-enhanced chemical vapor deposition. The plasma provides the energy to dissociate the silane which initiates film growth, although the complex chemical process of deposition is still not completely understood. Films are usually grown at 200–300°C, and virtually any material that can stand this temperature is a suitable substrate, although glass is the most common. The reactor can be scaled to large size, and deposition systems with substrates measuring many square feet presently produce solar cells.

Amorphous silicon has standard semiconducting properties. It has an optical bandgap of about 1.7 eV, exhibits n-type and p-type doping by the addition of phosphorus- or boron-containing gases to the deposition reactor, and is highly photoconductive.[3] The material owes most of its useful properties (but also some problems) to the presence of about 10 at.% of hydrogen, which originates from the SiH_4 deposition gas. The hydrogen reduces the

E_g = 1.1eV for single xtalline Si.

mobility gap 1.85eV

Table I: Some Typical Room-Temperature Electrical Properties of Hydrogenated Amorphous Silicon, as Compared to Crystalline Silicon.

	a-Si:H	Crystalline Si
Electron mobility	1 cm^2/Vsec	1300 cm^2/Vsec
Hole mobility	3×10^{-3} cm^2/Vsec	500 cm^2/Vsec
n-type conductivity	$10^{-2}\Omega^{-1}cm^{-1}$	$10^{2}\Omega^{-1}cm^{-1}$
p-type conductivity	$10^{-4}\Omega^{-1}cm^{-1}$	$10^{2}\Omega^{-1}cm^{-1}$

Density of states $D(E)$ is still a valid concept.

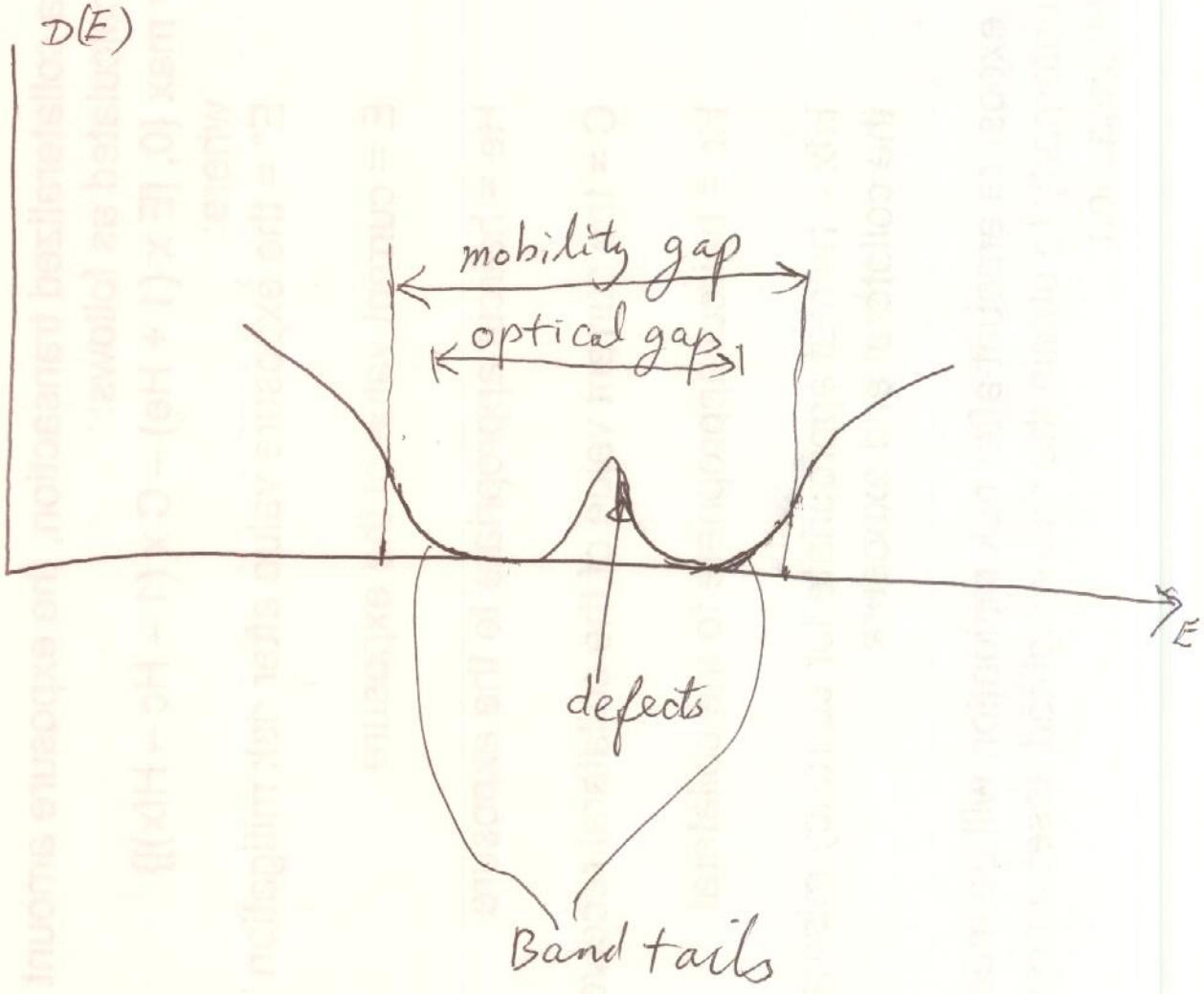

Extended states & localized states

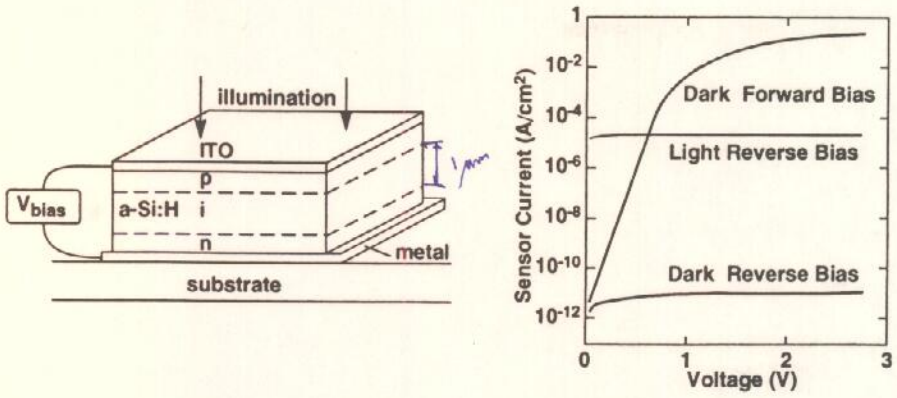

Figure 2. Structure of the n-i-p sensor and its electrical characteristics in forward and reverse bias.

density of electronic defects formed by silicon dangling bonds to about 10^{15} cm^{-3}. The atomic structure in Figure 1 illustrates the disorder and the hydrogen bonding.

Devices made from a-Si:H are designed around the specific material properties, particularly of the doped films. Although a high concentration of impurity dopant atoms can be introduced into a-Si:H, the effectiveness of doping is low. The doped material has a higher defect density than undoped a-Si:H, reaching above 10^{18} cm^{-3} for 1 at.% dopant incorporation and these act as compensation centers. In addition, not all the impurity atoms are active dopants, and the fraction decreases at increased concentrations. The conductivity of doped a-Si:H is further reduced by the low carrier mobility, which is a consequence of both the frequent scattering by the atomic disorder and the presence of localized trapping states near the band edge. Table I compares the electronic properties of amorphous and crystalline silicon. Although the electronic properties are clearly much poorer in the amorphous state than in the crystal, they are sufficient for the needs of most matrix-addressed arrays.

Like most materials, a-Si:H has its problems. A particular concern for many device applications is its inherent structural instability, first observed as a light-induced increase in defect density that caused solar cells to degrade slowly during operation.[4] This effect is caused by the migration of hydrogen, which creates dangling bond defects as it detaches from a Si-H bond. The instability is induced by the presence of nonequilibrium carriers and is therefore a potential problem in any electronic device. Fortunately, the effect occurs very slowly at room temperature and hardly interferes with the matrix-addressed arrays, although it limits their operation to below 50°C. Much of this materials research effort is aimed at mitigating the instability problem.

Sensors and Transistors

Optical sensors and field effect transistors are the two important active devices used in the array technology. Both have structures generically similar to their crystalline counterparts, although the details of the design are tailored to the material properties. The usual sensor structure, shown in Figure 2, is an n-i-p device in which the undoped i-layer is about 1 μm thick and the doped n- and p-layers are about 10 nm. The high-defect density of doped a-Si:H makes it insensitive to light, as compared with the undoped layer. The doped layers are therefore present only to provide an electrical junction with low reverse bias leakage current, and are made as thin as possible to avoid optical absorption losses. Fortunately, the same high-defect density gives them a small depletion layer width, and a 10-nm film is sufficient.

The low carrier mobility of a-Si:H suppresses diffusion currents in the undoped layer and efficient charge collection requires an internal electric field. Undoped a-Si:H has a depletion width of about 1 μm at zero bias, placing an upper limit on the thickness of solar cells. A reverse bias extends the depletion layer, even up to 50–100 μm, but present array processing technology limits the thickness to 1–3 μm, and such sensors exhibit full collection at a modest reverse bias (see Figure 2). The atomic disorder of a-Si:H eliminates the indirect bandgap of crystalline silicon, so that a 1-μm-thick film absorbs light across the whole visible spectrum, with its peak quantum efficiency reaching 90–95%, and conveniently centered at 500–600 nm.

The thin sensor has a capacitor structure and therefore provides its own storage of the light-induced charge. A sensor measuring 100×100 μm has a capacitance of about 1 pF and its charge storage capacity is equivalent to the charge generated by room-light exposure for about 0.1 msec.

The thin-film field effect transistor (TFT) is similarly designed around the specific electronic properties of a-Si:H. The undoped channel avoids the high defect density of doped material, and the TFT is operated under electron accumulation because the electron mobility is much higher than that of holes (see Table I). The usual gate dielectric is silicon nitride, which has the advantage of being deposited in the same reactor as a-Si:H by addition of NH_3 to the gas mixture. One of the common TFT structures is shown in Figure 3. The gate is deposited first, partly because the optimum growth temperature of the nitride is higher than of a-Si:H, and partly because a better interface results when the nitride is deposited first, for reasons that are poorly understood. The thin active layer of the TFT is typically about 50 nm, and the source-drain contacts are n-type a-Si:H, to give good electron injection and to block holes. A top nitride passivation layer prevents leakage along the top interface.

The electronic characteristics of the TFT

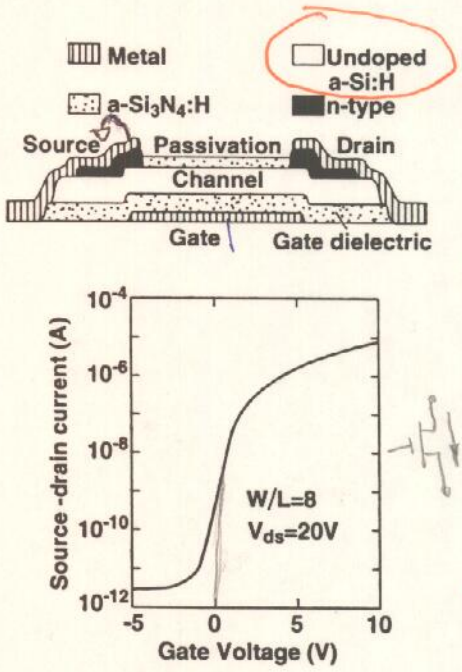

Figure 3. Structure of the field effect thin-film transistor (TFT) and its typical electrical transfer characteristics for a source-drain voltage of 20 V.

Polycrystalline Si ~ poly-Si

Higher mobility, both n- & p- channel devices available; higher temperature, higher cost.

Polycrystals, domains (grains), boundaries.

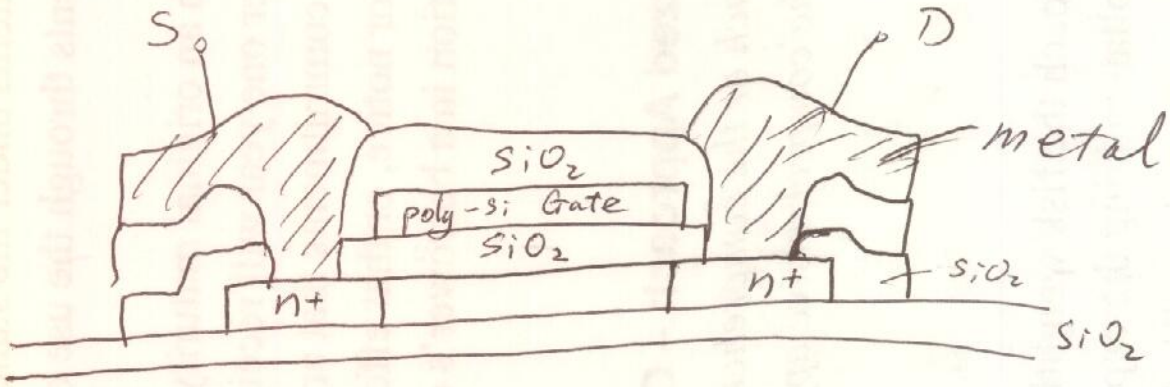

fused quartz

Fabrication:

SiO_2 Buffer layer: LPCVD/PECVD, 400°C; 500 nm

poly-Si channel precursor: " 350-550°C, 50-100 nm

" crystallization: Furnace 500-600°C, RTA, or laser

poly-Si island etch

Gate dielectric deposition: LPCVD/PECVD

Gate dielectric anneal: 600°C

Poly-Si gate deposition. LPCVD/PECVD 350°-550°C

" Etch

Organic TFTs (OTFTs)

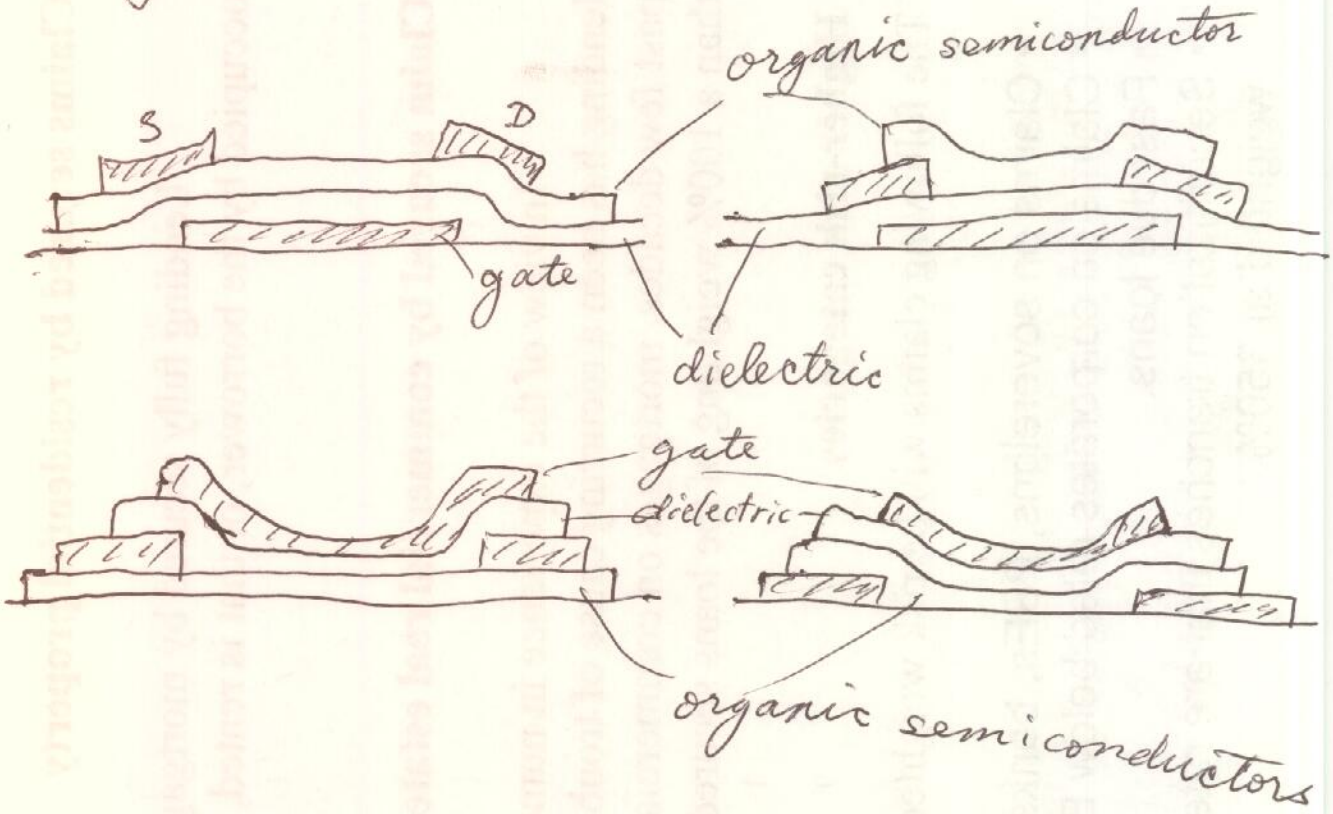

- Most organic semiconductors are sensitive to solvents — can't use photolithography.
- But patterning is needed. Often done w/ shadow masks during deposition
- Choice of device configuration often dictated by this limitation in patterning.
- S/D contacts formed by metals
  (No doping, no self-alignment)
  Choice of contact metal

Organic semiconductor channel materials.

Polycrystalline molecular thin films

small molecule example: pentacene

polymer example:

poly(3-hexylthiophene), P3HT

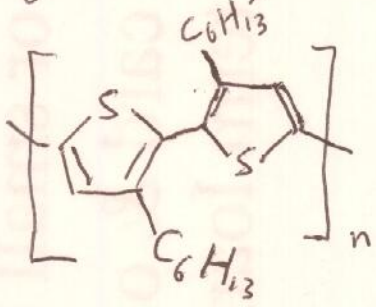

Organic Molecules – Electronic Structures, Properties, and Reactions

1 Introduction

Several chapters of this book describe the utilization of organic molecules for novel electronic devices: Carbon Nanotubes for Data Processing (Chap. 19), Molecular Electronics (Chap. 20), Neurobiological Interface (Chap. 32), Liquid Crystal Displays (Chap. 37), and Organic LEDs (Chap. 38). For this reason, here we give a very brief introduction to organic chemistry, focusing on the requirements of the devices chapters.

Section 2 summarizes the main classes of hydrocarbons and bond types, then Sec. 3 applies the methods of quantum mechanics (Chap. 3) to hydrocarbons. Finally, Sec. 4 introduces the functional groups and the major types of reaction mechanisms. Because space is limited, the reader should refer to the standard textbooks on organic chemistry and physical chemistry, for example, Refs. [1] – [6], in order to obtain a deeper understanding of the subject.

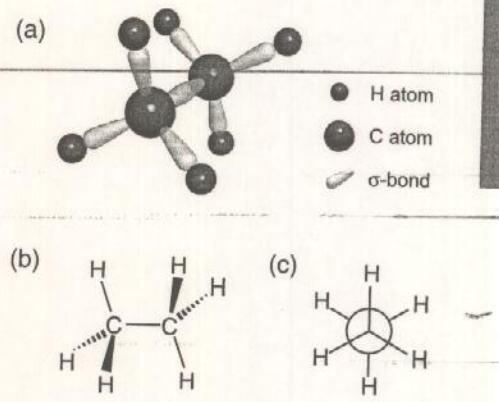

Figure 1: Representations of ethane, C_2H_6.
(a) Structural representation of the bonds.
(b) Sawhorse presentation.
(c) Stereo projection along the C-C axis.

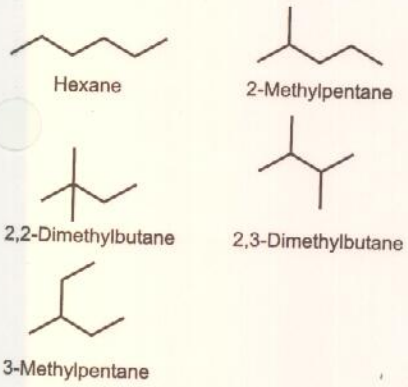

Figure 2: Structural isomers of hexane C_6H_{14}. According to the rules of the IUPAC (International Union of Pure and Applied Chemistry), the names of the isomers are based on the longest continuous carbon chain as the root, with branching groups named as substituents. The position in the root to which an alkyl group is attached is designated by number, starting at the end closest to the attachment. For this figure, the line notation of the organic chemistry is used. This notation represents C-C bonds by single lines. The presence of C-H bonds is inferred as needed to meet the valence requirements of carbon.

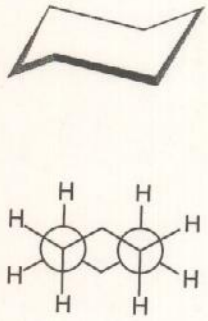

Figure 3: Structural representation of cyclohexane, C_6H_{12}.

2 Hydrocarbons

Saturated hydrocarbons are called **alkanes** and have molecular formula C_nH_{2n+2}. The chemical bonding in alkanes can be described as sp^3 hybridization of the atomic orbitals (AO) at the carbon atoms, corresponding to a tetrahedral arrangement of the σ-bonds with the neighboring C and H atoms. As an example, Figure 1 shows the configuration of ethane, C_2H_6. Free rotation is possible around the C—C σ-bond with an activation energy of about 0.1 eV. For alkanes with $n > 3$, there are structural **isomers** (different arrangements of the same numbers of atoms) in the form of chains and branched molecules, as illustrated in Figure 2 for hexane, C_6H_{14}. Alkanes with a ring-type structure are called **cycloalkanes**. Figure 3 shows the structure of cyclohexane, for example.

Hydrocarbons with C=C double bonds are called **alkenes**. The sp^2 hybridization of the carbon AOs corresponds to a trigonal planar configuration of the σ-bonds with the neighboring C and H atoms. The remaining p-AOs at neighboring C atoms take part in bonding, for which the electron density is not concentrated along the axis connecting the two bonded atoms as in the σ-bonds, but is located above and below the axis (Figure 4) with its plane of maximum electron density normal to the plane of σ-bonds. The length of a C=C double bond is 134 pm whereas that of a C-C single bond is

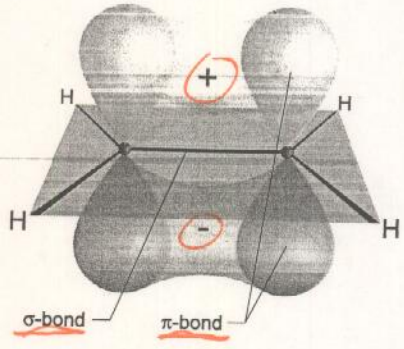

Figure 4: Illustration of the π-bond of ethene, C_2H_4, resulting from the co-planar p-AOs of the sp^2 hybridized C atoms. For clarity of the picture, the σ-bonds are not shown in their full shape.

Signs of the wavefunction not charge

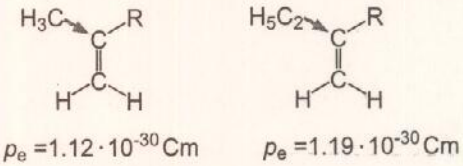

$p_e = 1.12 \cdot 10^{-30}$ Cm $\quad$ $p_e = 1.19 \cdot 10^{-30}$ Cm

Figure 5: Dipole moment for alkenes in which the double bond is located asymmetrically within the molecule.

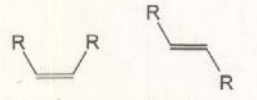

Figure 6: *Cis*- and *trans*-isomers of an alkene molecule. R indicates an alkyl substituent.

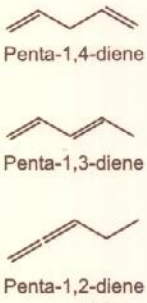

Figure 7: Types of polyenes illustrated by different pentadienes. Penta-1,4-diene shows isolated double bonds, penta-1,3-diene shows conjugated double bonds, and penta-1,2-diene shows cumulated double bonds. Since the C atom in the center of the cumulated double bond is sp-hydridized, this double bond is linear.

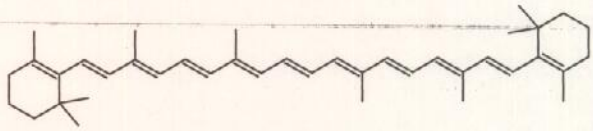

Figure 8: β-Carotene as an example for a polyene with long conjugated double bonding system.

σ - bonds form the skeleton of the molecule.

π - bonds are electronically active.

154 pm. In contrast to single bonds, free rotation is not possible for double bonds since this would require the breaking of the π-bond. The physical properties of alkenes, such as melting and boiling temperatures and solubilities in various solvents, are similar to those of the alkanes. However, whereas alkanes are virtually non-polar, i.e. they have zero permanent electric dipole moment, p_e, asymmetric alkenes are slightly polar. This indicates that alkyl groups exhibit a weak electron donating effect (+*I* effect, see below), as illustrated in Figure 5. When different groups are attached on each side of a double bond, we distinguish between *cis*- and *trans*-isomers (Figure 6).

If there are more than one C=C bond in a molecule, the compounds are called **polyenes**. Depending on the different relative positions of the C=C bonds, the bonds are referred to as isolated, conjugated, and cumulated as shown in the example of pentadiene in Figure 7. As will be discussed later, conjugated C=C bonds play an important role in electron conduction because π-electrons are delocalized over the entire extent of conjugation. β-Carotene is an example of a naturally occurring polyene (Figure 8), and contributes to the colour of vegetation.

Cyclic polyenes with conjugation that spreads over an entire ring of atoms sequence constitute the class of **aromatic** hydrocarbons, or **arenes**. If they are planar (which permits overlap of adjacent p-AOs) and possess $4n+2$ electrons with $n = 1, 2, \ldots$ in the π-system (the Hückel criterion of aromaticity), they exhibit a high energetic stability. The π-electrons are delocalized over the entire ring and single and double bonds can no longer be distinguished: one consequence is the identity of bond lengths round the ring. The most prominent and important representative is cyclohexa-1,3,5-triene, which is universally called benzene (Figure 9). The electronic structure and the origin of the stability of aromatic rings with six π-electrons (i.e. $n = 1$ for the Hückel criterion) as in benzene will be discussed in Sec. 3.2. The pronounced stability and the delocalization of the π-electrons is maintained for fused rings, the so-called **polycyclic aromatic molecules**, (Figure 10), and for smaller or larger rings provided the number of π-electrons is kept at six (an electron sextet). As examples of the latter, Figure 11 shows a cyclopentadienyl anion and a cycloheptatrienyl cation. In addition, azulene can be regarded as a fused-ring of a cycloheptatriene and a cyclopentadiene. The Hückel stability criterion based on electron sextets can be extended to heterosubstituents in the carbon ring as shown in Figure 12 for some common hexagonal and pentagonal ring systems.

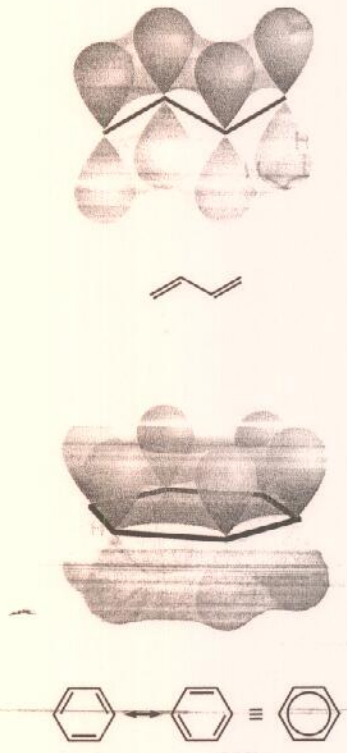

Figure 9: Structure and illustration of the electron density of the π-conjugated system of benzene. The two mesomeric Kekulé formulas according to the valence-bond theory as well as the frequently used Robinson ring symbol are shown.

Hydrocarbons with C≡C triple bonds are called **alkynes**. The C atoms participating in the triple bond are sp-hybridized and the bond consists of one σ-bond and two π-bonds. The σ-bond connecting triply bonded C atoms is surrounded by a cylindrical cloud of π-electron density (Figure 13). The bond length is 120 pm, which is shorter than for single and double bonds. Because of the linearity of a triple bond with its adjacent single bonds, no *cis/trans* isomerism exists. Conjugated triple bonds show the same electron delocalization as conjugated double bonds. Because of this delocalization and their simple linear structure they are sometimes regarded as rigid rods and are of great interest for molecular electronic systems.

Pentacene ultrathin film formation on reduced and oxidized Si surfaces

Ricardo Ruiz,[1] Bert Nickel,[2,3] Norbert Koch,[3,4] Leonard C. Feldman,[1] Richard F. Haglund,[1] Antoine Kahn,[3,4] and Giacinto Scoles[2,3]

[1]*Vanderbilt University, Department of Physics and Astronomy, Nashville, Tennessee, 37235*

[2]*Princeton University, Chemistry Department, Princeton, New Jersey, 08544*

[3]*Princeton Materials Institute, Princeton, New Jersey, 08544*

[4]*Princeton University, Department of Electrical Engineering, Princeton, New Jersey, 08544*

(Received 3 September 2002; published 12 March 2003)

We have compared the nucleation of pentacene on reduced and oxidized Si surfaces by a combination of x-ray reflectivity measurements and atomic force microscopy. For the reduced surface, the nucleation density is 0.007 μm^{-2}. Second monolayer (ML) formation starts at a coverage of $\Theta=0.6$ ML, and the first layer is completely closed at a total coverage of 2 ML. For the oxidized surface, the nucleation density is larger by a factor of 100 (0.7 μm^{-2}). Second ML formation also starts at $\Theta=0.6$ ML, but the first layer closes already at 1.1 ML coverage, indicating nearly ideal layer-by-layer growth. For both terminations, the electron density obtained for the closed first monolayer is only 75% of the bulk value, indicating a reduced mass packing efficiency of the layer. Second ML islands are aligned relative to each other on an area limited by the lateral size of first ML islands, which act as templates for epitaxial growth.

DOI: 10.1103/PhysRevB.67.125406 PACS number(s): 68.55.Ac, 61.10.Kw, 61.66.Hq

I. INTRODUCTION

Organic/inorganic interfaces are currently under investigation due to their critical role in molecular and bioelectronic technology.[1–3] Among the various materials being studied, pentacene ($C_{22}H_{14}$), a long, flat, aromatic molecule (see Fig. 1) is particularly promising for electronic applications. Pentacene forms good crystals if deposited onto flat, inert surfaces, resulting in highly anisotropic transport properties.[4] Pentacene is used to fabricate organic thin film transistors (OTFT's) in applications where large area coverage, mechanical flexibility, and room temperature processing are required.[5,6] In such devices, high field-effect mobilities up to 1.5 $cm^2/(V\,s)$[7] have been reported along with a variety of OTFT configurations and designs.[3,8,9]

Charge transport in an OTFT is confined to the first few monolayers in close proximity to the gate oxide (the channel).[10] Extensive work has been devoted to determine and optimize the charge transport properties of mesoscopic pentacene films (thickness range from 10 nm to 1 μm)[11–14] and to relate these properties to the crystalline structure and morphology. However, in order to disentangle structural aspects from fundamental limits of charge transport in organic materials, the confinement of the charge transport towards the gate oxide demands a detailed study of the early stages of film formation since these layers dominate charge transport.

In this paper we report a combined atomic force microscopy (AFM) and synchrotron x-ray reflectivity differential study of pentacene film formation on two different surface terminations [Fig. 1(e,f)] prepared by applying standard wet etching techniques to a thermally oxidized Si wafer. In our analysis, we focus on the coverage and structure of the first few monolayers. Our work is complementary to recent experiments, in which photoelectron emission microscopy (PEEM) demonstrated that pentacene film formation can be improved considerably by making use of a cyclohexane termination of clean Si(001) surfaces[15] or by means of hyperthermal beam-deposition energies.[16] Here, we demonstrate that similar full first layer coverage and layer-by-layer growth may also be achieved for clean oxide and H-terminated Si surfaces. We also demonstrate that different substrate terminations, having dissimilar surface energies, result in completely different morphologies and nucleation densities.

II. EXPERIMENTAL DETAILS

A. Substrate preparation

Since pentacene film formation is controlled by relatively weak van der Waals interactions, nucleation of the first monolayer (ML) is extremely sensitive to defects or impurities on the substrate surface which act as pinning centers. Heterogeneous surfaces lead to a wide range of morphologies and piling up of material, making the interpretation of properties, such as field effect mobility, difficult. To minimize the influence of surface impurities, we have applied the

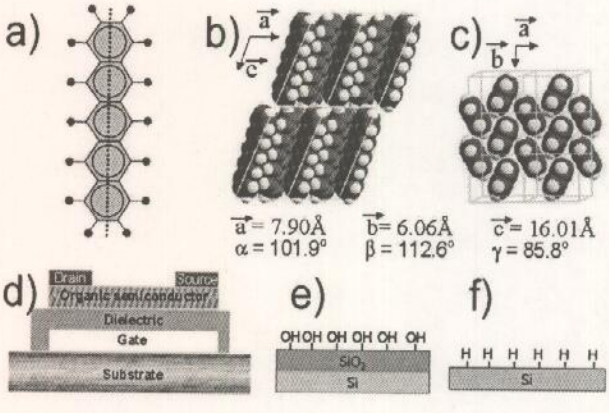

FIG. 1. (a) Molecular structure and (b) and (c) crystalline structure of pentacene. (d) Typical OTFT geometry (top contact), (e) O/OH terminated Silicon oxide, (f) H atom terminated Si.

 ©2003 The American Physical Society

Two-dimensional charge transport in self-organized, high-mobility conjugated polymers

H. Sirringhaus*, P. J. Brown*, R. H. Friend*, M. M. Nielsen†, K. Bechgaard†, B. M. W. Langeveld-Voss‡, A. J. H. Spiering‡, R. A. J. Janssen‡, E. W. Meijer‡, P. Herwig§ & D. M. de Leeuw§

* *Cavendish Laboratory, University of Cambridge, Madingley Road, Cambridge CB3 0HE, UK*
† *Condensed Matter Physics and Chemistry Department, Risø National Laboratory, 4000 Roskilde, Denmark*
‡ *Laboratory of Macromolecular and Organic Chemistry, Eindhoven University of Technology, 5600 MB Eindhoven, The Netherlands*
§ *Philips Research Laboratories, Prof. Holstlaan 4, 5656 AA Eindhoven, The Netherlands*

Self-organization in many solution-processed, semiconducting conjugated polymers results in complex microstructures, in which ordered microcrystalline domains are embedded in an amorphous matrix[1]. This has important consequences for electrical properties of these materials: charge transport is usually limited by the most difficult hopping processes and is therefore dominated by the disordered matrix, resulting in low charge-carrier mobilities[2] ($\leq 10^{-5}$ cm^2 V^{-1} s^{-1}). Here we use thin-film, field-effect transistor structures to probe the transport properties of the ordered microcrystalline domains in the conjugated polymer poly(3-hexylthiophene), P3HT. Self-organization in P3HT results in a lamella structure with two-dimensional conjugated sheets formed by interchain stacking. We find that, depending on processing conditions, the lamellae can adopt two different orientations—parallel and normal to the substrate—the mobilities of which differ by more than a factor of 100, and can reach values as high as 0.1 cm^2 V^{-1} s^{-1} (refs 3, 4). Optical spectroscopy of the field-induced charge, combined with the mobility anisotropy, reveals the two-dimensional interchain character of the polaronic charge carriers, which exhibit lower relaxation energies than the corresponding radical cations on isolated one-dimensional chains. The possibility of achieving high mobilities via two-dimensional transport in self-organized conjugated lamellae is important for applications of polymer transistors in logic circuits[5] and active-matrix displays[4,6].

We have studied the microstructure of 70–100 nm, spin-coated, regioregular P3HT films by grazing-incidence X-ray diffraction (XRD) on parts of the same SiO_2/Si substrates on which field-effect transistor (FET) devices were fabricated. Regioregularity denotes the percentage of stereoregular head-to-tail (HT) attachments of the hexyl side chains to the 3-position of the thiophene rings[7]. Two different orientations of the microcrystalline P3HT domains with respect to the FET substrate have been identified (Fig. 1). They are evident from the different intensity distributions of the (100) reflections due to the lamella layer structure and the (010) reflections due to π–π interchain stacking[8]. In samples with high regioregularity (>91%) and low molecular weight the preferential orientation of ordered domains is with the (100)-axis normal to the film and the (010)-axis in the plane of the film (Fig. 1a). In contrast, in samples with low regioregularity (81%) and high molecular weight, the crystallites are preferentially oriented with the (100)-axis in the plane and the (010)-axis normal to the film (Fig. 1b)[9]. The cause of this surprising change of orientation is not fully understood. It must be a dynamic phenomenon during the rapid growth of spin-coated films affected by either regioregularity or molecular weight. In films prepared by slow casting from a dilute solution the (100)-axis is normal to the film for all polymers (green trace in Fig. 1c and d).

However, the ability to induce different orientations allows us to establish a direct correlation between the direction of π–π stacking and the in-plane FET mobility μ (Fig. 2a). At room temperature the highest mobilities of 0.05–0.1 cm^2 V^{-1} s^{-1} are observed for the sample with the highest regioregularity (96%) and the largest size of crystallites with in-plane orientation of the (010)-axis (~95 Å, as estimated from (010) line shape analysis[10]). For spin-coated samples with HT ≈ 81%, in which the (010)-axis is normal to the film, the mobility is only 2×10^{-4} cm^2 V^{-1} s^{-1} in spite of pronounced in-plane crystallinity along the (100)-axis with a grain size of 130 Å. No clear correlation between FET mobility and weight average molecular weight M_w could be established, as seen previously between conductivity and M_w in highly doped P3HT (ref. 11). This is consistent with the FET mobility being limited by π–π interchain rather than intrachain transport as discussed below. In the case of the low-regioregularity polymers it is possible to directly compare mobilities for the in-plane (cast films) and out-of-plane orientation (spin-coated films) of the π–π stacking direction (Fig. 1d). In cast films of the 81% polymer the mobility is higher by more than an

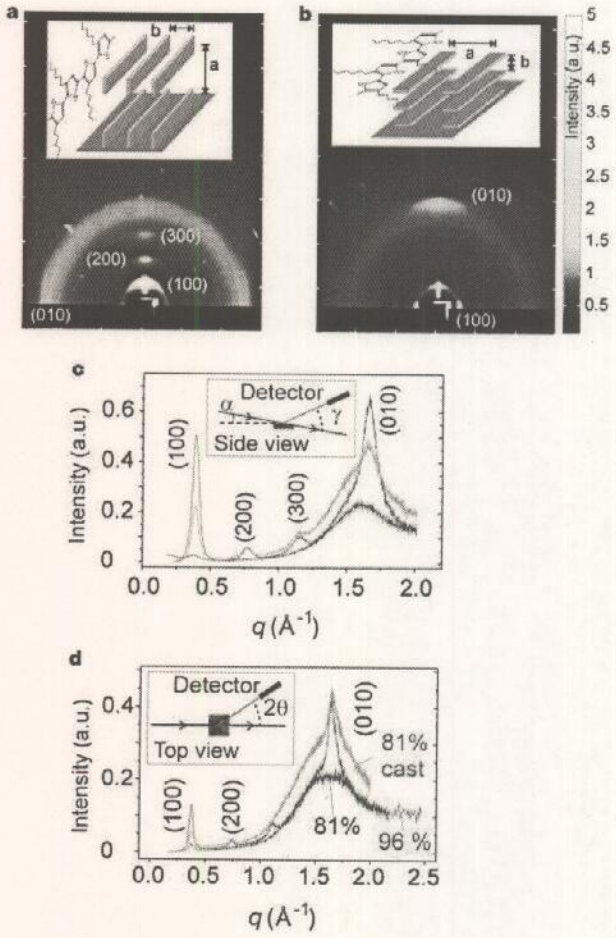

Figure 1 Two different orientations of ordered P3HT domains with respect to the FET substrate. **a**, **b**, The wide-angle X-ray scattering images are a colour representation of the two-dimensional distribution of scattered Cu Kα X-ray intensity from spin-coated, 70–100 nm thick P3HT films with regioregularity of 96% (**a**) and 81% (**b**) on SiO_2/Si substrates. The vertical (horizontal) axes correspond to scattering normal (parallel) to the plane of the film. The insets show schematically the different orientations of the microcrystalline grains with respect to the substrate. **c**, **d**, The change of orientation is confirmed by high-resolution synchrotron X-ray diffraction measurements for constant, grazing-incidence angle with out-of-plane (**c**) and in-plane (**d**) scattering geometry. Red, 96%, spin coated; blue, 81%, spin coated; green, 81%, solution-cast. The intensities plotted versus the total scattering vector are corrected for polarization and geometric factors[10].

© 1999 Macmillan Magazines Ltd

A quick, dirty lazy way to make a transistor
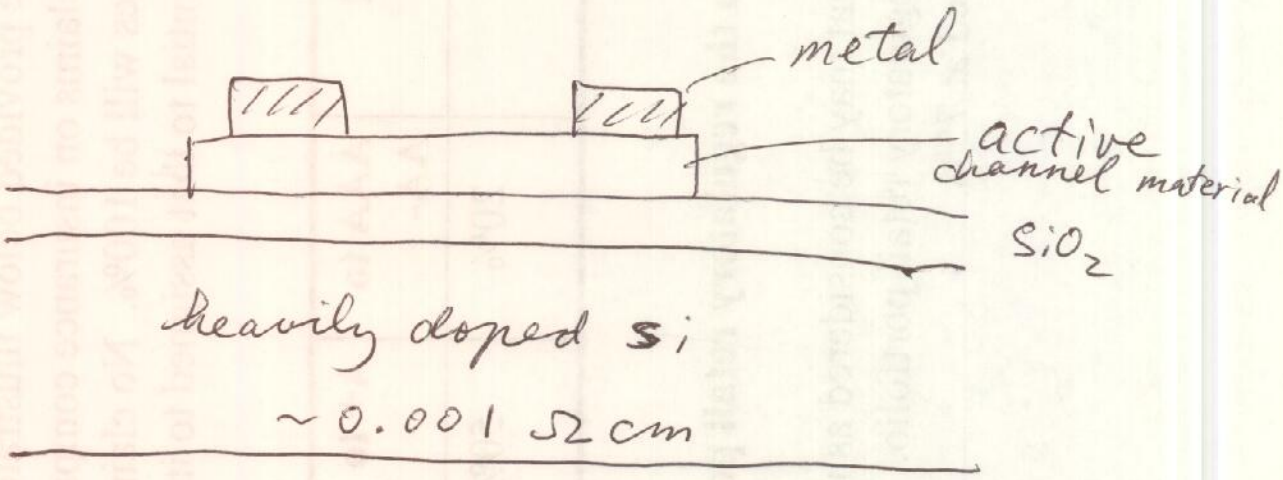
or not so dirty!